Journal of Catalysis **186,** 387–404 (1999)
Article ID jcat.1999.2561, available online at http://www.idealibrary.com on IDEAL®

A Molecular Beam Study of the Kinetics of the Catalytic Reduction of NO by CO on Rh(111) Single-Crystal Surfaces

Chinnakonda S. Gopinath and Francisco Zaera[1]

Department of Chemistry, University of California, Riverside, California 92521

Received February 23, 1999; revised May 6, 1999; accepted May 10, 1999

Steady-state rates for the catalytic reaction of NO with CO on Rh(111) surfaces have been measured under isothermal conditions by using a molecular beam approach with mass spectrometry detection. Systematic studies were carried out as a function of surface temperature, NO + CO beam composition, and total beam flux. A maximum in reaction rate was observed between 450 and 900 K, the exact temperature depending on the NO : CO beam ratio. Indeed, a synergistic behavior was seen where the loss in reactivity induced by increasing the CO concentration in the beam is partly compensated by a higher surface temperature. The data presented here are consistent with the rate-limiting step of the overall NO reduction process being the surface recombination of atomic nitrogen atoms resulting from fast dissociation of NO adsorbed molecules. Temperature-programmed desorption and CO titration experiments were also performed after the isothermal kinetic runs in order to estimate the surface coverages of the reactants during the steady-state reactions. The NO + CO conversion rate was found to be directly proportional to the coverage of atomic oxygen on the surface. The relation between reaction rates and nitrogen coverages, however, proved to be much more complex; an inverse correlation was in fact seen in most cases between those two parameters. The build-up of a critical coverage of atomic nitrogen was found to be necessary to trigger the nitrogen recombination step to N_2. This critical coverage of strongly held nitrogen was determined to not depend in any significant way on the composition of the beam, but to decrease with reaction temperature in all cases.

1. INTRODUCTION

The catalyzed reduction of nitric oxide to molecular nitrogen is critical in pollution-control processes for the treatment of combustion products from either automobile or stationary sources. The best answer available to date to the problem of the removal of air pollutants from the emission of such sources is the use of the so-called three-way catalytic converter (1, 2), a combination of palladium, platinum, and rhodium metal particles deposited on a high-surface-area support from which the use of rhodium in particular is essential because of its unique activity towards NO removal (1, 2). The conversion of NO to other innocuous gases is best accomplished by its reduction to N_2, a process that can be facilitated by the presence of a suitable reducing agent in the reaction mixture. Carbon monoxide is a particularly good candidate for this, since it is itself a contaminant produced by most combustion processes. NO reduction by CO occurs mainly through the overall reaction

$$NO + CO \rightarrow 1/2\ N_2 + CO_2. \qquad [1]$$

This paper is part of a continuing study in our laboratory to characterize the detailed kinetics and mechanism of this NO reduction on Rh(111) single crystals (3).

The reaction of NO with CO on rhodium surfaces has already been studied in some detail under vacuum (3–21). On Rh(111), early temperature-programmed desorption (TPD) experiments proved that Reaction [1] takes place even under vacuum (4, 5). It was also soon found that the key to understanding the details of the NO + CO reaction lies in the elucidation of the mechanism for the conversion of NO to N_2 on the surface. Interestingly, the desorption of molecular nitrogen from NO decomposition on Rh(111) occurs in two stages, around 470 K and above 500 K (3, 4, 22–25). The high-temperature peak of this nitrogen desorption follows a second-order kinetics easily explaind by assuming the recombination of nitrogen atoms on the surface as rate limiting. The first N_2 peak at 470 K, however, does not shift in temperature with changing coverages, a behavior generally associated with first-order processes. Even though surface-sensitive techniques such as X-ray photoelectron spectroscopy (XPS) (22), static secondary-ion mass spectrometry (SSIMS) (23), and high-resolution electron energy loss spectroscopy (HREELS) (24, 25) have been employed to show that NO dissociation occurs at quite low temperatures, below 300 K at low coverages and around 450 K at high coverages, it has nevertheless been argued that the rate-limiting step in the N_2 production on saturated surfaces could still be the dissociation of molecular NO, presumably because at high coverages the active sites for dissociation may be blocked by other absorbates (6, 26). There is, however, no conclusive evidence available to support this hypothesis.

[1] Corresponding author.

0021-9517/99 $30.00

The kinetics of the NO + CO reaction over Rh(111) has been studied at moderate pressures as well (10, 11, 17, 27). Interestingly, even though the commercial Rh/Al_2O_3 automotive catalysts produce N_2 exclusively over a wide range of operating conditions (15, 18, 20), the production of some N_2O was detected in the single-crystal studies (11). Fisher and co-workers (4, 5, 7–9, 24), in their initial studies in the mid-eighties, proposed two separate pathways for this, the generally accepted recombination of nitrogen atoms on the surface, and a disproportionation between adsorbed NO and N which could also account for the formation of the N_2O. Newer experimental data by Belton *et al.* (10, 11, 17, 26, 27), however, proved that the latter does not in fact occur on Rh(111), at least under vacuum. Clearly, the questions of the nature of the rate-limiting step and of the source of N_2O production are still open to debate.

In order to address these issues, we have carried out isothermal molecular beam kinetic experiments on the NO + CO reaction on Rh(111) single-crystal surfaces over a wide range of temperatures and reactant mixture compositions. In this paper we concentrate on the results from studies under steady-state conditions; the details of the transient behavior will be published elsewhere (28). A few surprising facts were brought out by our experiments. Specifically, a maximum in rate was seen for the NO + CO reaction rate at a temperatures somewhere between 450 and 900 K depending on the composition of the beam. It was also discovered that there is a need for the build-up of a critical coverage of nitrogen atoms on the rhodium surface before the start of the production of N_2. No N_2O formation was ever detected in our experiments; only the stoichiometric Reaction [1] was seen here. Based on this work, we propose that the rate-limiting step for the overall NO + CO process is the recombination of nitrogen atoms, but that the kinetics of that step is complex and cannot be described by a simple Wigner–Polanyi model.

2. EXPERIMENTAL

All the experiments reported here were performed in a 6.0 L stainless-steel UHV chamber evacuated with a 170 L/s turbo-molecular pump to a base pressure of about 2×10^{-10} Torr. This system is equipped with a UTI 100C quadrupole mass spectrometer, a sputtering ion gun, and a molecular beam doser. A detailed description of the doser setup and of its calibration has been given elsewhere (29, 30). Briefly, the doser, a 1.2 cm diameter array of parallel microcapillary glass tubes (10 μm in diameter and 2 mm in length) aimed directly at the surface, is connected to a calibrated volume via a leak valve and a second shut-off valve which isolates it from the main vacuum vessel. The beam flux is set by filling the backing volume to a specific pressure, which is measured by a MKS baratron gauge, and by adjusting the leak valve to a predetermined set-point. A total flux of 0.5 monolayers per second (ML/s) was used in all the experiments reported here unless otherwise specified. A movable stainless-steel flag is placed between the surface and the doser in order to intercept the beam at will. The contribution from the background to the measurements of the reaction rates was deemed by independent calibration experiments at less than 20% of that from the direct beam (29).

The solid sample, an approximately rectangular ($1.10 \times 0.56\ cm^2$) Rh(111) single crystal, was cleaned *in situ*, initially by Ar^+ sputtering and before each experiment by cycles of oxygen exposures (1×10^{-7} Torr at 900 K for up to 20 min) and annealing to 1200 K until the NO TPD spectra reported in the literature (3, 4, 23) could be reproduced. The crystal, which could be heated resistively or cooled by using a liquid nitrogen reservoir to any temperature between 90 and 1200 K, was placed at a distance of 0.5 cm from the front of the doser to assure a reasonably flat gas flux profile (29). The surface temperature was monitored continuously by a chromel-alumel thermocouple spot-welded to the back of the crystal, and kept constant during the kinetic runs with a home-made precision temperature controller. TPD spectra were recorded at a constant heating rate of 10 K/s. Isotopically labelled ^{15}NO (CIL, 98% ^{15}N purity) and regular CO (Matheson, 99.9% purity) were used as supplied. Since only ^{15}N-labelled nitric oxide was used in this work, we will refer to ^{15}NO, $^{15}N_2$, and ^{15}N simply as NO, N_2, and N, respectively, hereafter. The pressure of the gases in the vaccum chamber was measured with a nude ion gauge, and was calibrated for differences in ionization sensitivities (31).

The time evolution of the partial pressures of up to ten different species, including N_2O and NO_2, were followed simultaneously in both the isothermal kinetic runs and the TPD experiments by using the computer-controlled quadrupole mass spectrometer, which was placed out of the line of sight of both the beam and the crystal in order to avoid any artifacts due to possible angular profiles in either the scattered or the desorbing gases. The mass spectrometer signal for nitric oxide was calibrated by equating the time-integrated ^{15}NO uptake on clean Rh(111) at 200 K to its saturation coverage, which was assumed to be 0.7 monolayers (ML) (4, 22, 23). The nitrogen signal was then calibrated by using the relative mass spectrometer sensitivities for ^{15}NO and $^{15}N_2$, and independently by mass balance arguments (and the assumption of a constant NO sticking coefficient at low coverages in the TPD experiments (3)). Similar considerations were applied for the CO calibration, for which the saturation coverage was assumed to be 0.75 ML (32).

3. RESULTS

3.1. General Considerations

The experimental procedure used here for the rate determinations in the NO + CO/Rh(111) system is based on

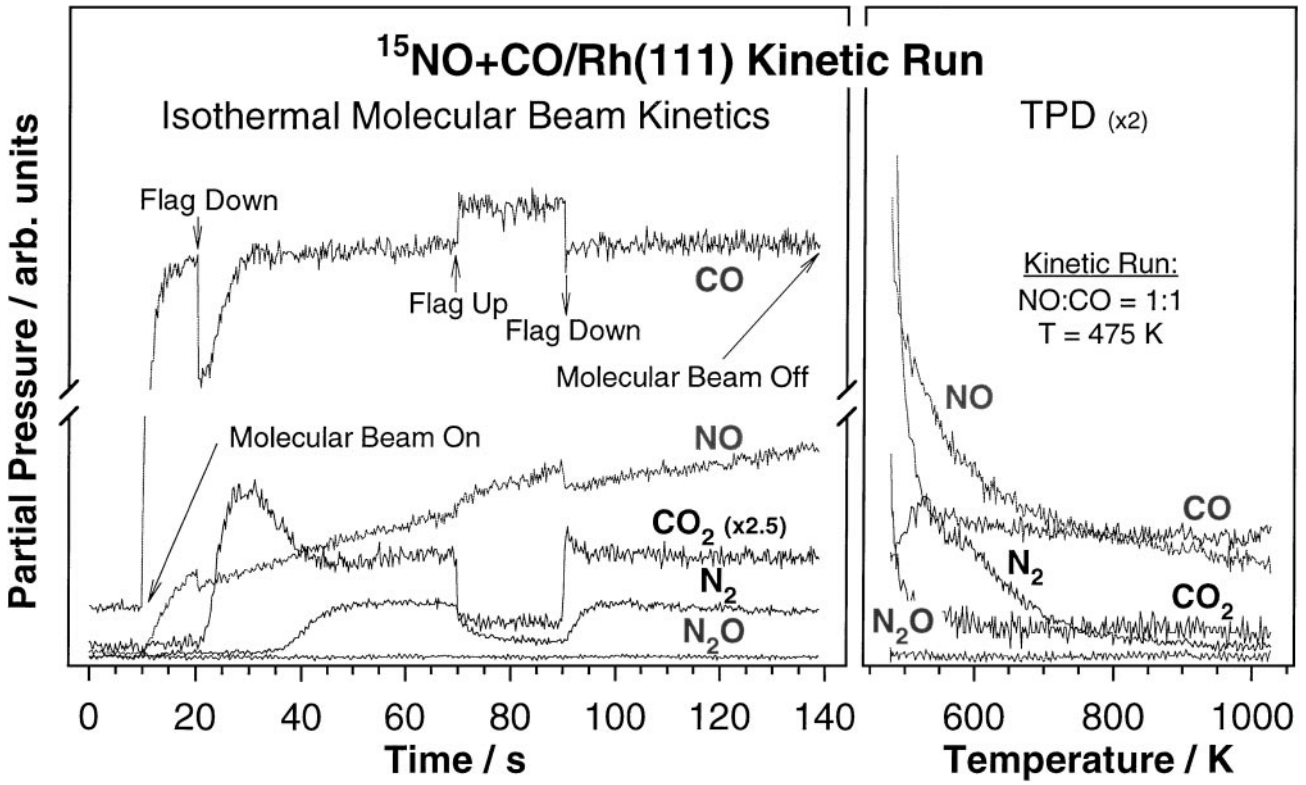

FIG. 1. (a) Raw data from a typical isothermal kinetic run of the type described in this report. In this case an effusive 1 : 1 $^{15}NO + CO$ collimated molecular beam was directed onto a clean Rh(111) surface kept at 475 K while the partial pressures of $^{15}N_2O$ (which was not produced at all here), $^{15}N_2$, CO_2, ^{15}NO, and CO were followed as a function of time. The beam was blocked between $t = 70$ and 90 s to measure the steady-state rate of the $NO + CO$ conversion. (b) Temperature-programmed desorption (TPD) spectra for the key species in the $^{15}NO + CO$ reaction after the isothermal kinetic run shown in (a). Heating rates of 10 K/s were used. Reaction rates and surface coverages were calculated by integration of the raw data from these experiments as described in the text.

exposing the clean rhodium surface, which is kept at a constant temperature, to an effusive collimated $NO + CO$ molecular beam of preset composition, and on following the partial pressure of the different gases of interest as a function of time by mass spectrometry (29, 30). As an example of the results obtained with this approach, the left panel of Fig. 1 shows the raw kinetic data for the evolution of the partial pressures of N_2O, N_2, CO_2, NO, and CO over time in the case of a 1 : 1 NO : CO beam composition ratio and a reaction temperature of 475 K. A series of actions are taken during these experiments as follows: (1) At time $t = 10$ s the $NO + CO$ molecular beam is turned on with the flag in the intercepting position so the crystal is not yet exposed directly to the beam. At this point the reactant molecules (NO and CO) are scattered throughout the vacuum chamber, so their partial pressures increase up to new steady-state values. Notice that the partial pressure of CO_2 does increase somewhat at this point too because of the reaction between the background NO and CO on the Rh(111) surface (this represents less than 20% of the total rate, and was included in the data analysis (3, 33)). (2) At approximately $t = 20$ s the flag is removed from the path of the $NO + CO$ beam in order to allow for its direct impingement on the surface. This causes both a decrease in the partial pressures of the reactants as well as an increase in the signals of the products. This stage will be termed here as the "transient state," and will not be discussed in detail in this publication. Notice that while a change in the CO_2 signal is seen immediately after the unblocking of the beam, the signal for the formation of N_2 rises only after a delay of about 20 s from that point. (3) The system is allowed to evolve until a steady state is reached, which in general happens within 50 s after the unblocking of the beam. Neither the adsorption of the reactants nor the desorption of the products changes with time in this steady-state condition. The continuous rise of the NO partial pressure beyond this point is due to poor pumping speed for this compound from the vacuum chamber, and does not represent any chemical change in the system. (4) During the steady-state regime the molecular beam is blocked deliberately by raising the flag (at time $t = 70$ s in this example) to check on the values of the reaction rates. There is a clear increase in the partial pressure of the reactants and an accompanying drop in the partial pressure of the products at that point, and

a new steady-state is reached within a few seconds of this beam blocking. (5) After about 20 s from the blocking of the beam, i.e., at $t = 90$ s, the flag is removed again and the reaction is allowed to return to the earlier steady-state regime induced by the direct impingement of the beam on the surface. (6) At about $t = 200$ s the molecular beam is turned off to stop the reaction. (7) After the partial pressures of reactants reach their initial background levels, the crystal temperature is lowered below 250 K, and the surface is saturated with CO if titration of the O atoms left on the surface is to be performed. (8) Finally, the crystal temperature is ramped at a constant rate of 10 K/s to record the TPD traces for CO and NO (to measure the amount of any unreacted molecules), CO_2 (from CO + O recombination), N_2 (from N + N recombination), and O_2 (from O + O recombination). The results from this last step are shown in the right panel of Fig. 1. The CO_2 (from the titration experiments) and N_2 TPD traces in particular allow for the calculation of the coverages of O and N atoms that remain on the surface after stopping the steady-state reaction. One final note about this figure: the trace for N_2O (46 amu) shows no features anywhere during the kinetic runs, indicating that no N_2O is produced at any stage in these experiments. This was true for all the data shown in this paper.

A systematic set of steady-state kinetic studies for the NO + CO reaction on Rh(111) was carried out as a function of surface temperature, NO : CO ratio, and total beam flux by following the procedure described in the previous paragraph. The partial pressures of the different gases were then converted into reaction rates by following a calibration procedure described in previous publications (29, 33). As an example of the results of these calculations, Fig. 2 displays the typical temporal evolution of the calibrated reaction rates for the uptake of NO and for the desorption of the products (CO_2 and N_2) during the steady-state part of an experiment carried out at 500 K with a 1 : 7 NO : CO beam ratio. Note that the rate for the NO uptake (0.0141 ± 0.0010 ML/s) is almost equal to that for CO_2 production (0.0137 ± 0.0010 ML/s), and is close to two times that for N_2 formation (0.0056 ± 0.0005 ML/s), the proportions expected by the stoichiometry of the overall Reaction [1]. This stoichiometry was found to hold for most of the reaction conditions used in our experiments (see below).

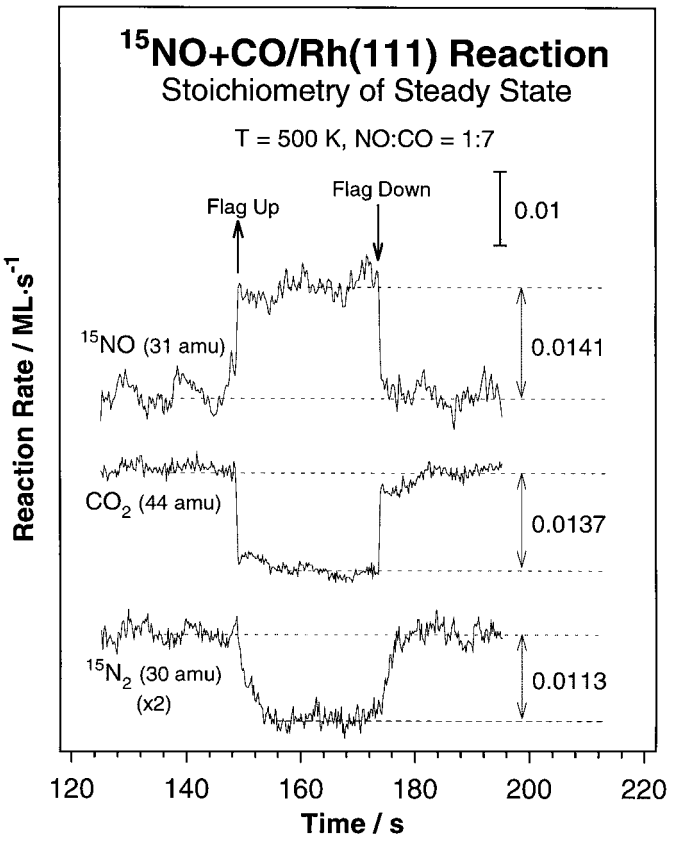

FIG. 2. Measurement of the steady-sate reaction rates for the consumption of ^{15}NO and for the production of $^{15}N_2$ and CO_2 at 500 K with a 1 : 7 NO : CO beam. The absolute values of the rates in ML/s were calculated by the calibration experiments discussed in the text. This figure shows the stoichiometric nature of the $NO + CO \rightarrow 1/2\ N_2 + CO_2$ reaction.

3.2. Temperature Dependence

Figure 3 displays the time evolution of the steady-state rates of production of CO_2 (left panel, a) and N_2 (right panel, b) during the isothermal exposure of the Rh(111) surface to a 1 : 7 NO : CO beam at different crystal temperatures. It is seen here that no significant NO conversion can be catalytically sustained at temperatures below 400 K, as expected based on previous TPD results (3, 4). Above 450 K, however, the steady-state rates for the production of both N_2 and CO_2, which are proportional to the changes in partial pressures between the flag up and flag down times, increase rapidly with temperature until reaching a maximum value at about 600 K. Notice also that the kinetics observed in these transients to the new steady state (immediately after the changes in the flag position) are quite different for N_2 and CO_2, because while CO_2 reaches its new steady state instantaneously (within the time resolution of our experiments) upon blocking and unblocking of the beam, the N_2 desorption rate decays more slowly as the beam is intercepted, and, similarly, the rise in the N_2 partial pressure to the earlier steady-state level is not immediate but takes a few seconds after the flag is again removed from the path of the beam. The main conclusion from this observation is that the recombination of nitrogen atoms must be rate limiting for the whole process under the conditions of those experiments. Finally, for the case of the 1 : 7 of NO : CO beam composition used in Fig. 3, the rate for the NO + CO reaction decreases sharply above 600 K, and is no longer limited by the N + N recombination step above 800 K.

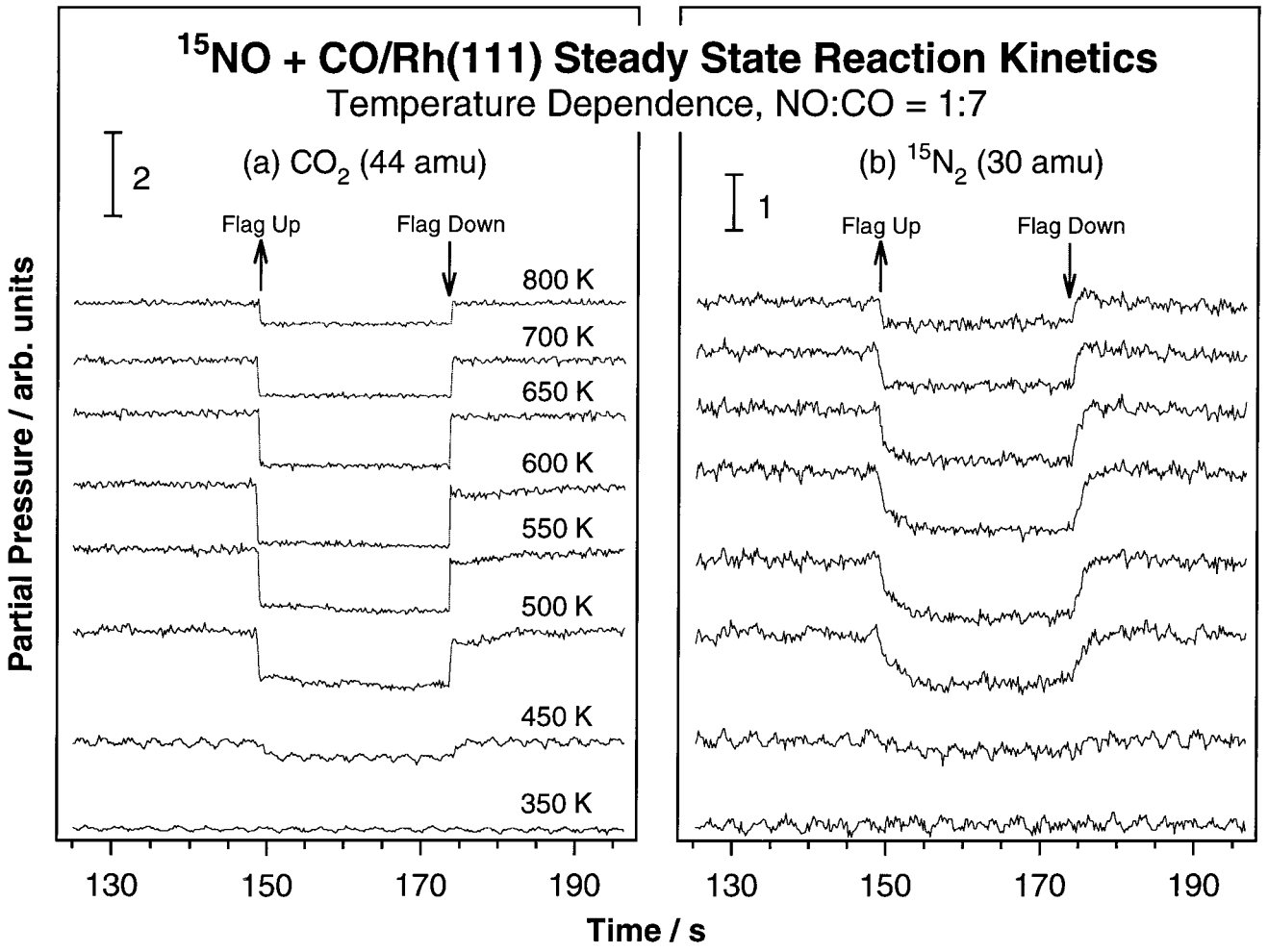

FIG. 3. Time evolution of the partial pressures of the products, CO_2 (a) and $^{15}N_2$ (b), in steady-state kinetic experiments with a 1:7 $^{15}NO:CO$ beam as a function of surface temperature. The rate-limiting nature of the N recombination step is illustrated by the slow kinetic behavior of the N_2 evolution at the points where the beam was blocked and unblocked.

A summary of the reaction rates measured as a function of temperature for the CO_2 and N_2 production and for the NO uptake in the case of the 1:7 NO:CO beam composition is shown in Fig. 4. All these rates are believed to be accurate to within 10%, the main source of systematic errors originating from the mass spectrometer calibration and the contribution of the background gases to the overall measured reaction rates and reactant uptake. In relative terms, the reported values were reproducible to within 5% for a given beam composition, beam flux, and surface temperature. Figure 4 corroborates that the overall reaction rate increases with increasing temperature until reaching a maximum at 600 K and decreases again afterwards, and it also confirms the stoichiometry of the reaction by illustrating that the rates for NO consumption are basically the same (within experimental error limit) as those for CO_2 production and about twice those for N_2 desorption at all temperatures.

3.3. Composition Dependence

Figure 5 shows the kinetic traces obtained for the NO + CO reaction in the steady-state regime at a constant temperature, 500 K, for NO:CO ratios ranging from 4:1 to 1:99. The general description given for Fig. 3 is applicable to this figure as well. Of note here is the fact that when the beam is rich in NO (for instance, in the case of the 4:1 NO:CO composition) the rate of the overall reaction is low even at surface temperatures high enough to dissociate NO molecules, but as the beam is made richer in CO the NO + CO steady-state reaction rate increases rapidly until reaching a maximum at an approximately equimolar NO:CO composition. Also, in addition to the almost instantaneous response of the CO_2 rate to the blocking of the beam, the N_2 decay is also reasonably fast for the stoichiometric (1:1) mixture. With CO-rich beams (for NO:CO ratios above 1:15), the excess CO renders the reaction

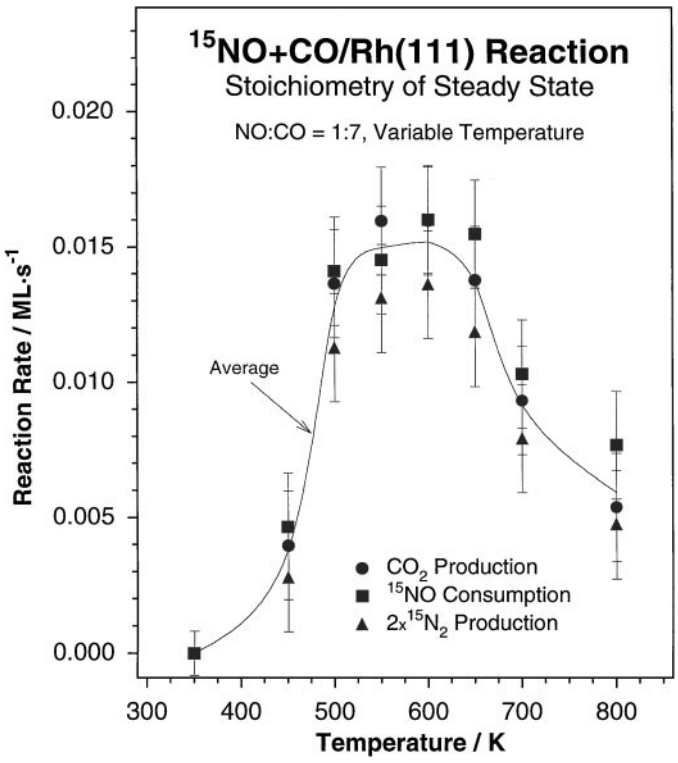

FIG. 4. Temperature dependence of the rates of ^{15}NO consumption and of $^{15}N_2$ and CO_2 production in the steady-state regime for a 1 : 7 ^{15}NO : CO beam, as extracted from the data in Fig. 3. The stoichiometry of the reaction is maintained, within an error of less than 10%, over the whole temperature range studied. The solid line does not represent any fit to the data and is provided only as guide to the eye.

quite inefficient once again. Two more observations are worth mentioning from this figure: (1) The CO_2 trace always shows an immediate drop right after the molecular beam is blocked, but a further slow decay in signal continues for some time thereafter in the case of the 1 : 3 NO : CO mix (a similar instantaneous increase in the CO_2 partial pressure followed by a further slow growth for another 10 s or so is seen in that case when the molecular beam is unblocked). (2) The N_2 trace displays slower responses at the flag up and flag down points as the beam is made richer in CO.

3.4. *Synergism between Temperature and Composition for Rate Changes*

Figure 6 provides a summary of the results obtained in the steady-state kinetic experiments reported here in terms of the overall NO + CO reaction rate against both reaction temperature (left panel) and beam composition (right panel) for a series of initial settings. These rates were calculated by averaging those for the formation of CO_2 and N_2 (times two), namely,

$$R = \frac{R_{CO_2} + 2 \cdot R_{N_2}}{2}. \qquad [2]$$

A few interesting points are worth highlighting from this figure: (1) There is an optimum reaction temperature, somewhere between 450 and 900 K, where a maximum in rate is reached for a given NO : CO beam composition. (2) The above optimum temperature shifts to higher temperature with increasing CO (and/or decreasing NO) content in the reaction mixture. (3) There is also an optimum NO : CO ratio, somewhere between 1 : 1 and 1 : 7, which maximizes the reaction rate. The exact value of this ratio again depends on the reaction temperature. (4) The overall steady-state reaction rate is the highest (about 0.02 ML/s) for a temperature of 550 K and a 1 : 3 NO : CO beam composition. (5) There is a general broadening in the temperature range where the reaction rate displays appreciable values (relative to the maximum) as the beam becomes richer in CO. For instance, in the case of the 1 : 7 NO : CO beam, similar reactivity is seen between 550 and 600 K, while with a 1 : 32 NO : CO ratio, the region where comparable rates are observed widens to between 500 and 800 K (these changes may alternatively be viewed in terms of a lesser sensitivity of the reaction rates to beam composition at high temperatures). All of the above observations demonstrate that the reaction rate is effectively controlled by both the surface temperature and the beam composition. In fact, it appears that the effect of increasing the reaction temperature can be compensated to some extent by a decrease in the concentration of NO in the beam: For example, almost the same rate is observed for beam compositions of 1 : 1 and 1 : 3 (NO : CO) at 500 and 550 K, respectively, and similarly, almost the same rate is observed at 450 and 800 K for 1 : 3 and 1 : 15 NO : CO beam compositions, respectively.

3.5. *Flux Dependence*

Figure 7 shows the results from studies on the changes in reaction rate (R) as a function of NO flux (F_{NO}) in a beam of fixed 1 : 7 NO : CO composition. For all the F_{NO} values used here the rate follows, within experimental error, the same trend as in Fig. 4, namely, it increases up to about 600 K and drops afterwards. R also increases with increasing flux (Fig. 7, right panel), but not in a linear fashion as expected. Moreover, the rate of nitrogen production displays two distinct regions in the transient right after the blocking of the beam (Fig. 7, left panel): There is a sharp initial drop within the first couple of seconds after the flag is moved into the intercepting position, which appears to scale reasonably well with the total flux of the beam, implying that the rate at that point is proportional to F_{NO} (and possibly to Θ_{NO}), but there is also a second slower region after that where the N_2 formation rate displays similar behavior regardless of the total flux of the beam. This second regime could perhaps be due to reactions involving background gases, since it was found that the background pressure of reactants in the steady state is significant compared to the flux from the direct molecular beam in the case of low-flux beams

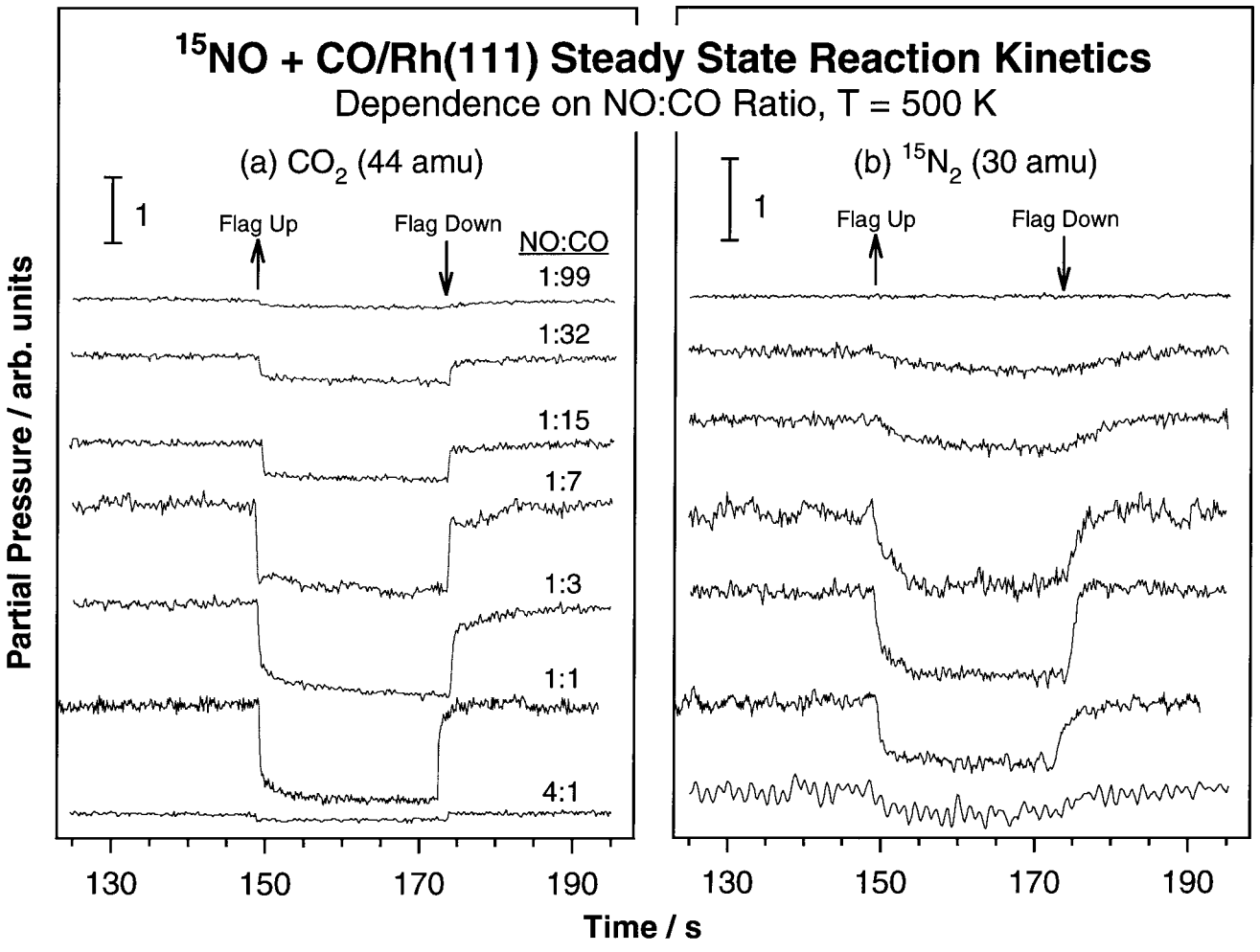

FIG. 5. Time evolution of the partial pressures of the products, CO_2 (a) and $^{15}N_2$ (b), in kinetic steady-state experiments at 500 K as a function of $^{15}NO:CO$ beam ratio. Again, the fast response observed in the CO_2 desorption traces at the blocking and unblocking of the beam contrasts with the slower kinetic behavior seen for N_2.

but does not increase substantially in absolute terms with increasing beam flux (amounting to less than 10% of the total impinging molecules for $F_{NO} = 0.20$ ML/s). Most of the experiments reported in this paper were carried out with reasonably high-flux ($F_{total} = 0.5$ ML/s) beams in order to minimize this effect.

3.6. Surface Coverages under Reaction Conditions

The coverages of the various species present on the surface under steady-state conditions were determined by TPD experiments carried out after the isothermal kinetic runs. Figure 8 shows the N_2 TPD traces obtained from the Rh(111) surface after performing NO + CO reactions with a beam of 1 : 7 NO : CO composition at different temperatures. The N_2 desorption in these TPD experiments comes from recombination of the N atoms strongly bonded on the surface (Θ_N^{strong}), which, as argued below, are required before any N_2 production can be seen during the steady-state conditions (34). The shape of these traces are basically the same as those in TPD experiments from Rh(111) dosed with either NO (3–5, 22–25) or N_2 (26, 35), indicating that the kinetics of desorption in this case is controlled by the atomic nitrogen recombination step, and their areas (which are proportional to Θ_N^{strong}) decrease monotonically with increasing reaction temperature. Notice the two distinct states that develop at high coverages after low-temperature (350 K) reactions, as mentioned in the Introduction.

The coverages of surface oxygen (Θ_O) present during the steady-state reaction conditions were determined by post-mortem CO titration experiments. For this, the Rh(111) surface was cooled to 250 K after the stopping of the NO + CO reaction and then saturated with CO before the CO_2 TPD traces were obtained. It is important to note that since CO desorbs at temperatures close to those at which CO_2 is produced, oxygen removal by this method can sometimes be incomplete. Since the oxygen coverages in these experiments are low, however, there was no problem with the

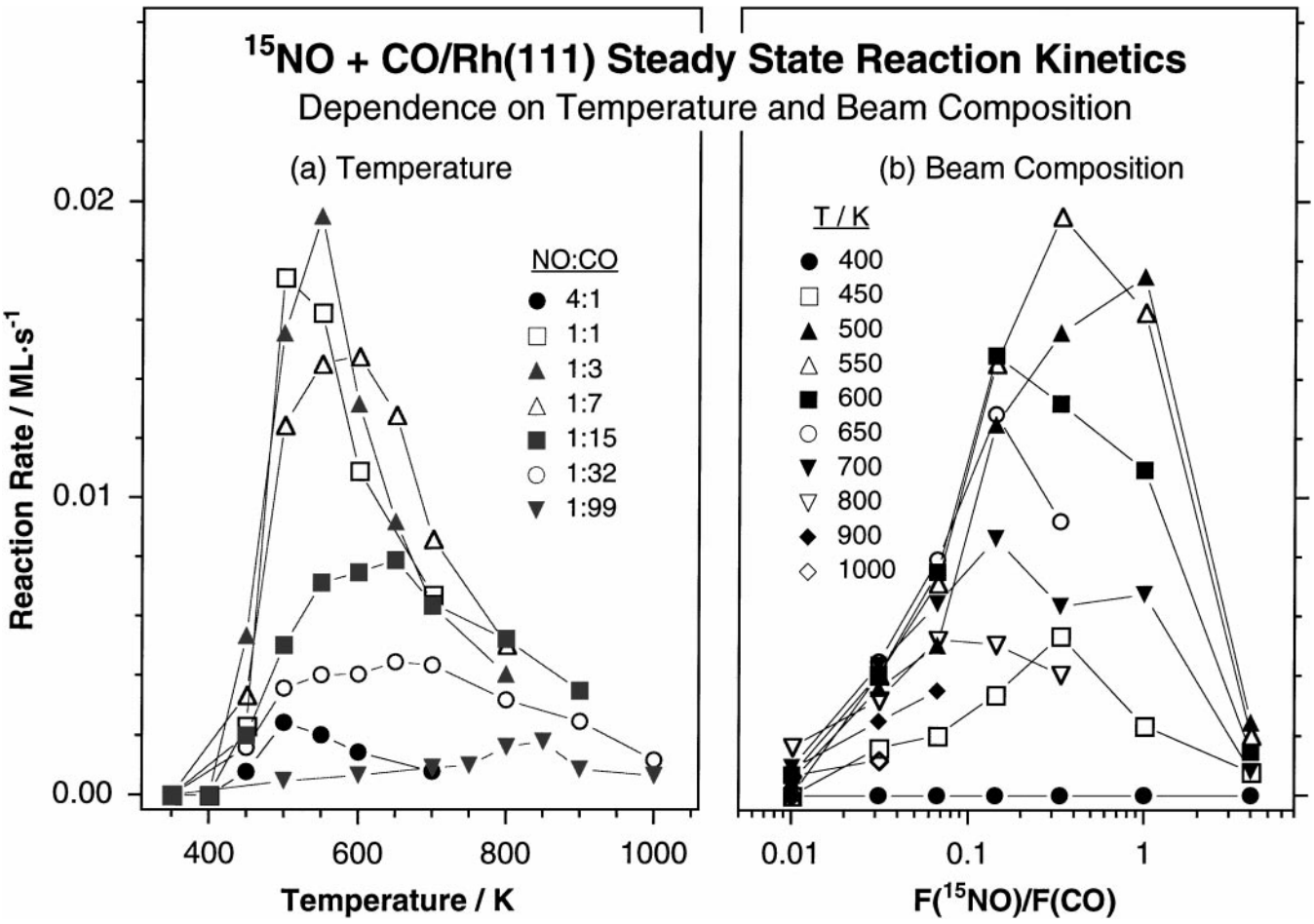

FIG. 6. $^{15}NO + CO$ reaction rates both as a function of temperature for $^{15}NO:CO$ beam ratios between 4:1 to 1:99 (a) and as a function of beam composition for temperatures between 400 and 1000 K (b). The maximum in reaction rate shifts to higher temperatures with increasing CO concentration in the beam.

stoichiometry of the CO titrations, as checked by two independent tests, namely, by comparing with direct O_2 TPD data (which yielded similar results but were less reliable) and by performing a second CO titration experiment immediately after the first.

The three panels in Fig. 9 show typical CO titration TPD results for NO:CO ratios of 1:3 (a), 1:7 (b), and 1:15 (c) and a number of reaction temperatures between 340 and 800 K (no CO post-dosing was carried out after the kinetic experiments done at 340–350 K, since no CO desorption takes place at those reaction temperatures). It can be seen from these data that for reaction temperatures of 400 K and above small amounts of O atoms may be present on the surface, the actual oxygen coverage depending on the beam composition (especially on the concentration of CO in the beam). The data also provide information on the nature of the atomic oxygen present on the surface during the NO + CO reactions. Notice in particular that after reactions at temperatures below 600 K the CO_2 TPD titration traces display significant signals only above 400 K irrespective of the beam composition, but that for reaction temperatures above 650 K the CO_2 TPD show an additional and distinct desorption peak at a lower temperature, about 360 K. The relative intensity of this new feature varies with reaction temperature: it develops suddenly between 650 and 700 K and disappears again at 800 K in the TPD from CO-rich beams, for 1:7 NO:CO beam ratios and lower (Fig. 9b), but it becomes less significant for the 1:3 NO:CO case. All this can roughly be explained in terms of isolated versus islanded oxygen atoms on the surface (36), even though a more detailed analysis is hindered by the fact that some CO and O_2 desorb above 1100 K in TPD performed after the high-temperature (>700 K) reactions, suggesting that subsurface oxygen may also form on the Rh(111) substrate.

As mentioned before, below 400 K almost all surface sites are blocked within a few seconds after the start-up of the reaction, most likely with CO and NO, and no steady-state reactivity can be sustained. Indeed, the TPD traces obtained after exposures of the surface to the NO + CO beam at 350 K yielded large amounts of N_2 (equivalent to

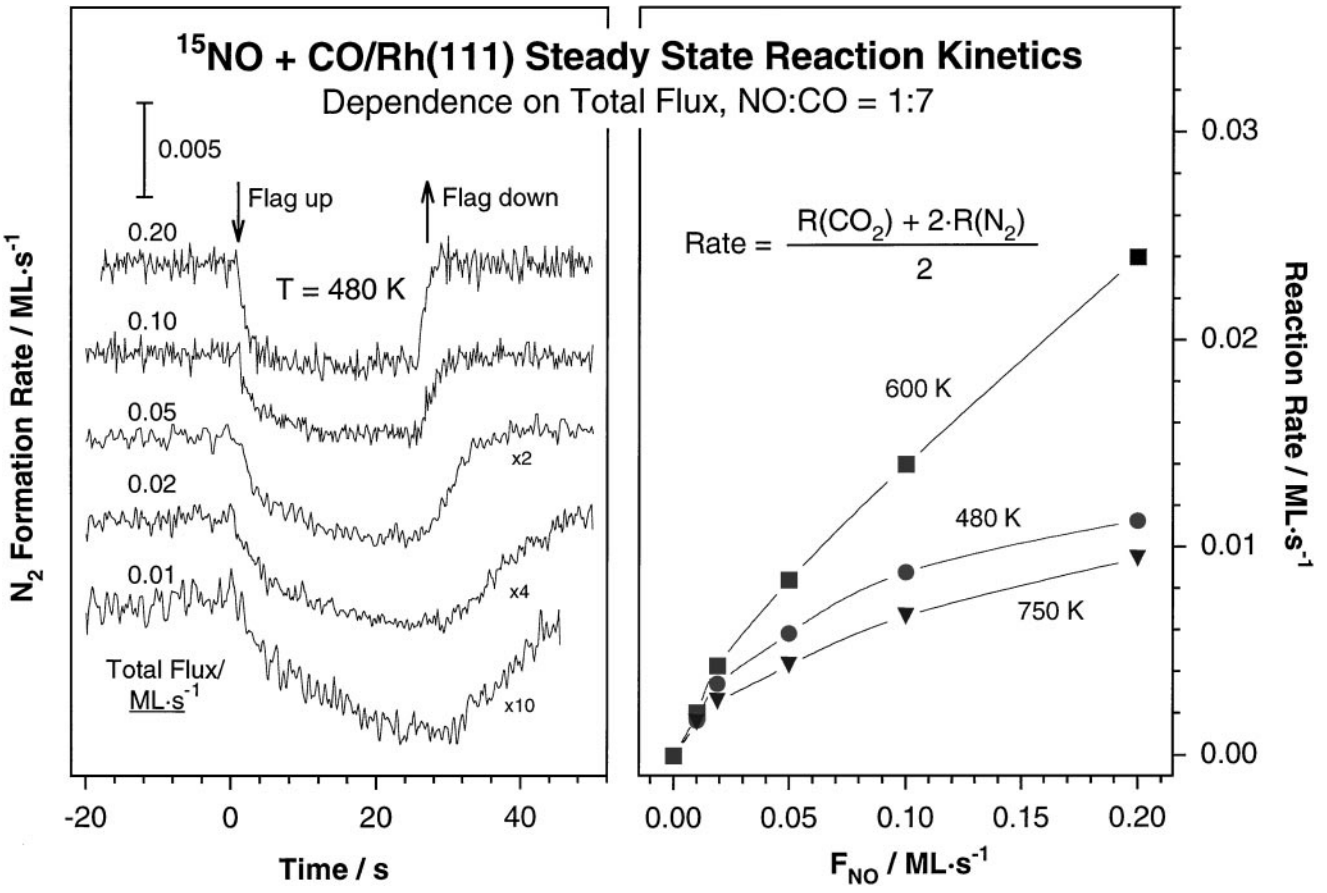

FIG. 7. (a) Time evolution of the $^{15}N_2$ formation rate at 480 K for a 1 : 7 ^{15}NO : CO beam as a function of total beam flux. The immediate decay from the steady-state nitrogen production rate after the blocking of the beam roughly scales with beam flux, but the second slower region that evolves afterwards probably reflects the conversion of background gases. (b) $^{15}NO + CO$ conversion rates at 480, 600, and 750 K as a function of ^{15}NO flux. Significant deviations from linearity between reaction rates and beam fluxes are seen here, especially for temperatures distant from the optimum 600 K value.

$\Theta_N = 0.48$ ML for the 1 : 7 NO : CO composition) and CO_2 (equivalent to $\Theta_O = 0.12$ ML) as well as some unreacted CO ($\Theta_{CO} = 0.11$ ML) and NO ($\Theta_{NO} = 0.08$ ML). Figure 10, which displays the coverages of CO and NO that remain on the Rh(111) as a function of beam composition after a reaction temperature of 350 K, shows that with NO-rich beams (1 : 1 NO : CO) the surface is covered with NO exclusively, but that with increasing CO concentration in the beam the Θ_{NO} decreases gradually at the expense of an increase in Θ_{CO}. An almost equal coverage of CO and NO is seen on the surface at a NO : CO beam ratio of 1 : 7, and by a value below 1 : 15 almost no NO is detected in the TPD experiments. In terms of the temperature dependence of this competition between NO and CO adsorption, NO + CO uptakes at 375 K lead to the build-up of about the same Θ_{NO} but less Θ_{CO}, and by 400 K Θ_{NO} decreases to a maximum value of about 0.05 ML with NO-rich beams while Θ_{CO} goes down to 0.02 ML with CO-rich beams. These data indicate that NO adsorption is slightly favored on Rh(111) at low temperatures (when competing with CO), but that desorption and/or decomposition reduces the surface coverages of both NO and CO molecular species above 350 K.

Figure 11 summarizes the regular and CO-titration TPD results in terms of the surface coverages of O and N atoms under steady-state conditions between 350 and 1000 K for the various NO : CO ratios employed in the experiments reported here. As mentioned before, a simple general trend is seen in the coverage of N atoms as a function of temperature which holds true irrespective of the composition of the beam, namely, large Θ_N^{strong} values, on the order of half a monolayer, are seen on the Rh(111) surface at low temperatures (below about 500 K), but a sharp decrease in that coverage is observed with increasing reaction temperature until becoming almost negligible above about 600 K. In terms of the oxygen coverages, a careful look at the data reveals another clear trend, at least for beam compositions near the stoichiometric ratio (NO : CO = 1 : 1, 1 : 3, and 1 : 7), where Θ_O increases monotonically from 400 to about 650 or 700 K and then decreases abruptly to values close to zero above 900 K. For the intermediate 1 : 15 NO : CO beam

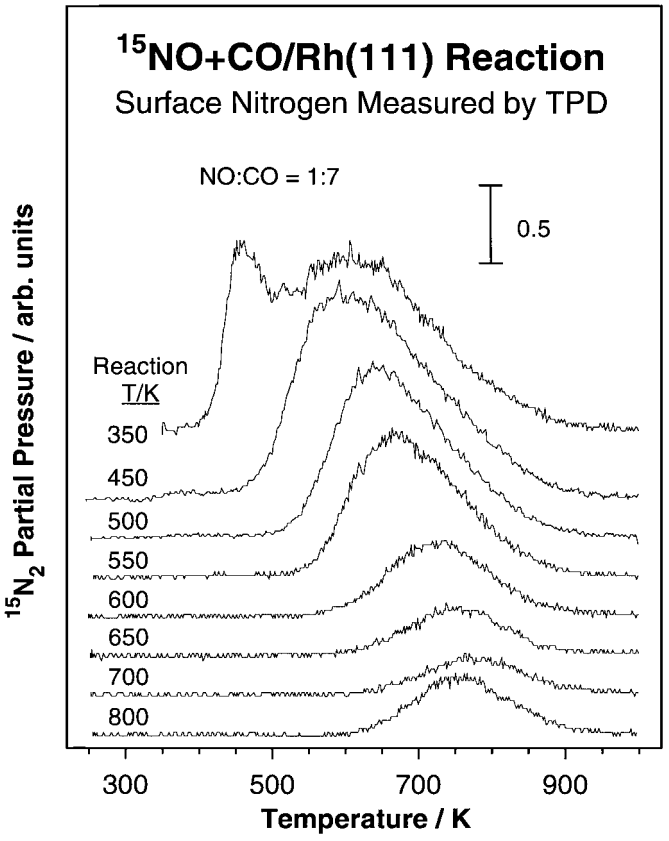

FIG. 8. $^{15}N_2$ TPD spectra obtained after the isothermal runs shown in Fig. 3. The coverage of strongly adsorbed nitrogen during the $^{15}NO + CO$ catalytic reactions, estimated from the areas under these traces, decreases abruptly with increasing reaction temperature.

some oxygen ($\Theta_O \sim 0.1$–0.2 ML) is seen between 700 and 800 K, but with either NO-rich (4 : 1) or CO-rich (1 : 32 and 1 : 99) beams, the oxygen coverage is quite low (≤ 0.05 ML) at all temperatures between 450 and 1000 K. The overall behavior of the coverage of oxygen during the NO + CO reaction can in most cases be explained by the efficiency with which CO removes O atoms from the surface via the formation of CO_2 and/or by the diffusion of oxygen atoms into the bulk (see below).

Figure 12 displays the dependence of the steady-state values of Θ_O, Θ_N^{strong}, and R as a function of beam composition for three key reaction temperatures, namely, 500 (a), 600 (b), and 700 (c) K. These results have already been reported above, but are displayed in a new way here to highlight the correlation between surface coverages and reaction rates. This figure shows that: (1) For a given beam composition the coverage of adsorbed oxygen atoms generally increases with reaction temperature. (2) A direct correlation exists between reaction rates and oxygen coverages, at least for NO : CO ratios below 1 : 3. (3) Larger Θ_N^{strong} values are seen with NO-lean beams at low temperatures, below 600 K, while the opposite trend is observed at 700 K. (4) Θ_N^{strong} generally decreases with reaction temperature for a fixed-beam composition, as shown earlier (remember that it is the nitrogen that does not react but needs to accumulate on the surface before a steady-state reaction can start). (5) A particular combination of high Θ_O and low Θ_N^{strong} values is seen with the 1 : 3 beam composition at all temperatures, especially when compared to the behavior of other beams with nearby compositions. Since this is the composition which leads to the highest NO + CO conversion rates, it is concluded that setting up the reaction conditions so as to maintain high Θ_O and low Θ_N^{strong} is essential to optimize the rate for NO reduction.

3.7. Relative Rates for CO Desorption and CO_2 Formation

Finally, in order to understand the processes responsible for the removal of surface oxygen at high temperatures, a few simple CO oxidation reactions were carried out on oxygen-treated Rh(111) surfaces between 300 and 700 K. Figure 13 displays the raw data from isothermal kinetic runs for the CO uptake on clean Rh(111) (top) as well as for the CO uptake (middle) and the CO_2 evolution (bottom) on oxygen-saturated Rh(111) at 300 (a), 450 (b), and 600 (c) K. The oxygen-saturated surfaces were prepared by dosing the rhodium substrate with 200 L (1 L = 1×10^{-6} Torr s) of oxygen at 600 K, a treatment that results in a (2×2)O–Rh(111) ordered surface (37). At 300 K CO adsorption takes place until saturation on both surfaces, as indicated by the dips in the corresponding traces (Fig. 13a) as the flag is removed from the beam ($t = 0$ s), but at 450 K a detectable amount of CO is adsorbed only on the clean surface, and no uptake is seen at 600 K even on clean Rh(111) because at that temperature the rate of desorption is high and a low and undetectable steady-state CO coverage is reached almost immediately after the dropping of the flag. The importance of these results to the understanding of the NO + CO reaction is that there is no appreciable effective CO uptake on the oxygen-precovered Rh(111) at temperatures higher than 450 K, and that the CO desorption rate above 450 K is much larger than that of the CO + O recombination step. Subsequent TPD experiments (data not shown) corroborated that indeed most of the predosed oxygen remains chemisorbed during isothermal exposures to the CO beam. This is in sharp contrast with the case of Pt(111), where the opposite is true (38).

4. DISCUSSION

4.1. General Considerations

The kinetic data presented here provide new information on the mechanism of the catalytic reduction of NO by CO over rhodium surfaces. There has already been a large amount of surface-science work done over the last two decades both on the dissociation of NO (3, 4, 7, 22, 23, 25, 39) and on its reaction with CO over Rh surfaces

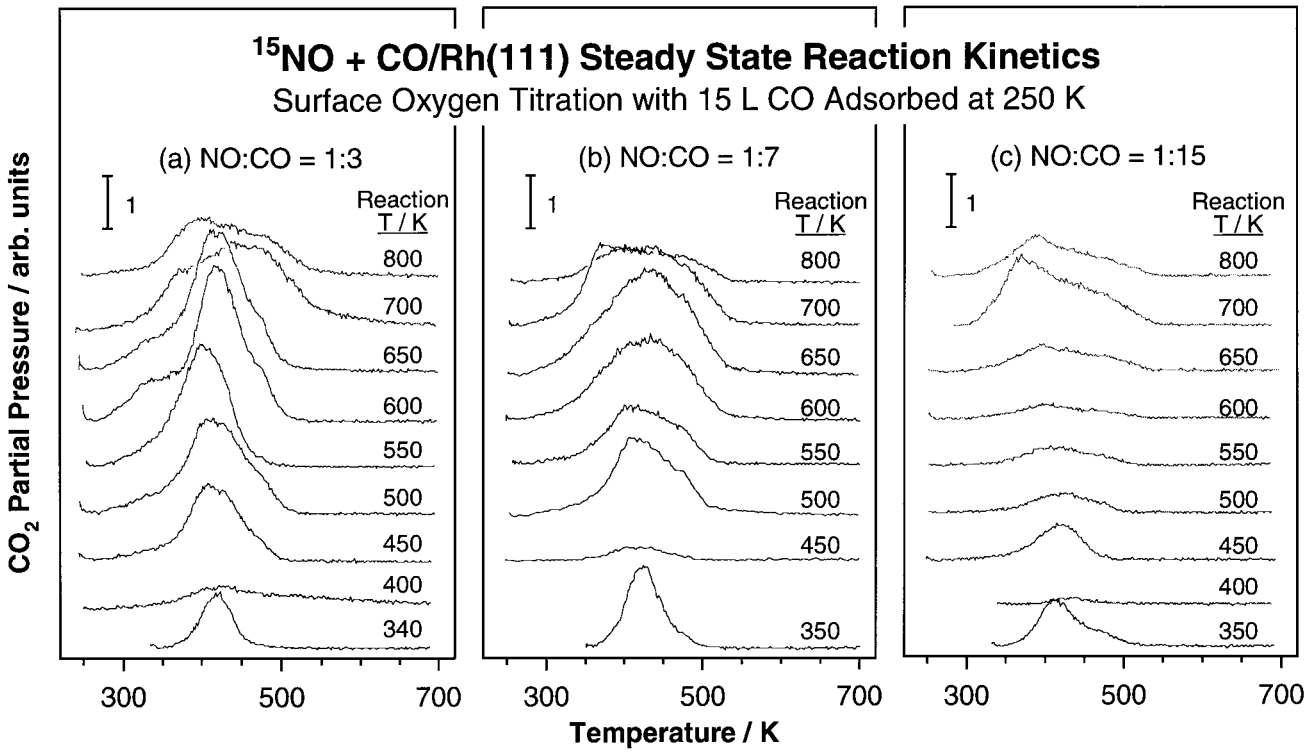

FIG. 9. CO_2 TPD traces from oxygen-titration experiments as a function of reaction temperature for 1:3 (a), 1:7 (b), and 1:15 (c) $^{15}NO:CO$ beam compositions. For these the surface was saturated with CO at 250 K after the isothermal kinetic runs. The areas under the CO_2 TPD peaks are used to determine the oxygen coverages on the surface during the steady-state reactions, and the observation of distinct CO_2 desorption peaks provides additional information on the nature of the surface oxygen atoms.

(5, 6, 8, 9, 11–14, 16). The following mechanism has been put forward for the NO + CO conversion:

$$CO(g) \rightarrow CO(ads) \quad [3]$$

$$CO(ads) \rightarrow CO(g) \quad [4]$$

$$NO(g) \rightarrow NO(ads) \quad [5]$$

$$NO(ads) \rightarrow NO(g) \quad [6]$$

$$NO(ads) \rightarrow N(ads) + O(ads) \quad [7]$$

$$2\,N(ads) \rightarrow N_2(g) \quad [8]$$

$$CO(ads) + O(ads) \rightarrow CO_2(g) \quad [9]$$

$$NO + CO \rightarrow 1/2\,N_2 + CO_2 \quad \text{overall reaction} \quad [1]$$

The first piece of evidence from our work in support of such a mechanism comes from Fig. 4, which provides data to establish that, at least under the conditions of our experiments, the NO + CO reaction is stoichiometric, meaning that for every two molecules of NO consumed, two molecules of CO are also converted, and two molecules of CO_2 and one molecule of N_2 are produced. No evidence was obtained here for the production of N_2O either as an intermediate or as a desorption product (Fig. 1). Hence, any N_2O-forming steps will be ignored in the remainder of this discussion.

One of the main points of contention in the literature with respect to the NO + CO reaction mechanism relates to the reaction rate-limiting step. As mentioned in the Introduction, the decomposition of adsorbed NO molecules on the rhodium surface has been recently proposed as such a step, at least under moderate and high pressure (6, 10, 17, 27). We will, however, argue below against the validity of this conclusion under vacuum. In connection with this, we will highlight the importance of a few observations deriving from our experiments, namely: (1) the almost immediate response of the rate of CO_2 production (via CO + O recombination) to any perturbation of its steady-state condition; (2) the slow kinetics of N_2 production irrespective of NO concentration in the reactant mixture, at least below 700 K, as manifested by the slow response of the rate of N_2 production to changes in the molecular beam flux; (3) the need to build up a critical nitrogen coverage on the surface before the start of the production of N_2; and (4) the often inverse correlation between the threshold nitrogen coverage and the NO reduction rate. These observations support the idea of nitrogen recombination to N_2 with a complex kinetic behavior as rate limiting the overall NO + CO conversion.

We start our discussion by providing a brief summary of the information available in the literature about the individual steps in the mechanism given above. First, the

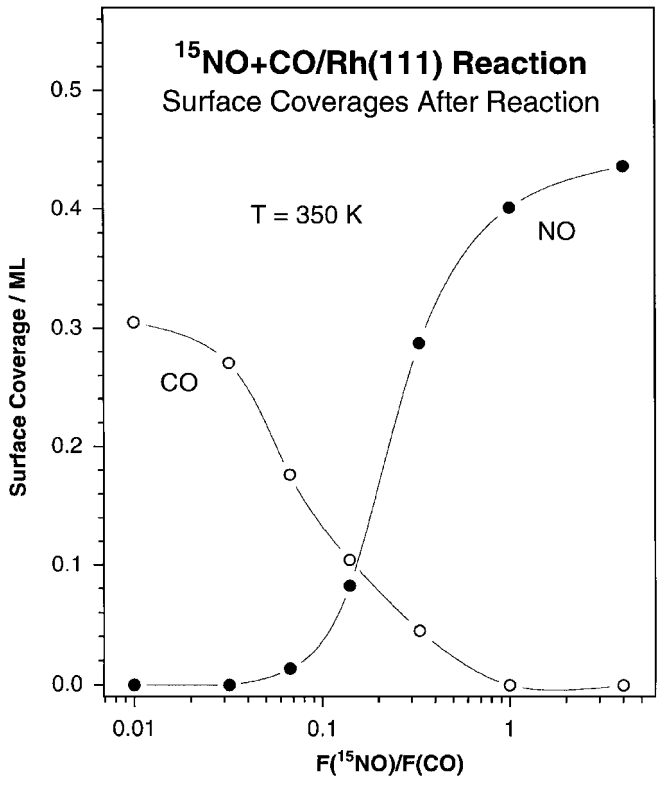

FIG. 10. ^{15}NO and CO surface coverages after kinetic runs at 350 K as a function of ^{15}NO : CO beam composition. The data show that CO-rich beams (NO : CO ratios of approximately 1 : 7) are required to achieve stoichiometric NO + CO adsorbed mixtures on the surface.

adsorption of CO, step [3], appears to be quite similar on Rh(111), Pd(111), and Pt(111) surfaces (29, 40). In particular, vibrational studies of CO on the Rh(111) surface show molecular adsorption, exclusively on linear sites at low coverages but on additional bridge sites at saturation (32, 40–42). In terms of the kinetics of the CO adsorption on Rh(111), measurements by Thiel *et al.* (32) and Peterlinz *et al.* (43) indicate that the CO sticking coefficient s_{CO} is constant for coverages up to about 0.3–0.5 ML, at which point it drops abruptly until reaching a value of zero at saturation. Like on other noble metals, the temperature dependence of s_{CO} on Rh(111) is weak; s^0_{CO} is in fact reported to be temperature independent between 320 and 400 K (43). With respect to CO desorption, step [4], TPD spectra show a single molecular desorption peak at 510 K up to moderate coverages and a shoulder around 425 K at high coverages (5). No CO decomposition occurs on this surface. Oxygen coadsorption does not affect the adsorption of CO on Rh(111) in any significant way (5, 36), but there is a repulsive interaction between CO and NO which leads to a decrease in CO desorption temperature in NO + CO coadsorbed systems (4, 7).

The initial sticking coefficient of NO on Rh(111), step [5], is high ($s^0_{NO} \sim 0.8$) and almost constant with temperature up to 800 K (3, 23). At 100 K NO adsorption shows an approximately constant s_{NO} with coverage up to $\Theta_{NO} = 0.5$ ML followed by a sudden drop at saturation, a behavior typical of precursor-mediated adsorption (3, 23), but at 300 K the uptake kinetics is more of the Langmuir–Hinshelwood type. A combination of vibrational and LEED studies suggests that at 100 K the NO adsorbs molecularly and on bridge sites (24, 25), but SSIMS data for the NO/Rh(111) system at 250 K is more in tune with NO occupying only three-fold sites at low coverages and additional bridge positions above 0.35 ML (23). Our earlier work on the uptake of NO on Rh(111) indicated that the kinetics of NO adsorption is not affected significantly by the presence of coadsorbed N and/or O atoms at any temperature below 900 K (3).

About the kinetics of NO desorption from Rh(111), TPD experiments indicate that at low temperatures (<250 K) and low exposures (up to about 0.2 ML) all the NO molecules decompose completely to surface N and O atoms upon heating of the surface (step [7]), but that at higher coverages some molecular desorption occurs at 440 K (step [6]). Interestingly, the N_2 TPD spectra (by N recombination, step [8]) from this system show two peaks, the first of which grows but does not shift with increasing initial NO coverages, as if it were a first-order process (3–5, 22–25). Temperature-dependent SSIMS studies of NO adsorbed on Rh(111) indicated that below 0.2 ML NO dissociates by 350 K, but that near-saturation coverages the desorption of some molecular NO at 440 K is required before the remaining adsorbates decompose. Still, the above observations, which have been confirmed by XPS and HREELS studies (22, 24), imply that in steady-state reactions at temperatures above 450 K NO is expected to dissociate immediately upon adsorption; the coverages of the molecular reactants (NO and CO) on the surface are likely to be negligible under these conditions. Indeed, no desorption of NO or CO was detected after blocking of the beam during our steady-state kinetic runs, and no molecular species were seen in the TPD experiments performed afterwards.

Finally, TPD data from CO + NO coadsorbed on Rh(111) have identified the production of some CO_2 from recombination of CO and O (step [9]) between 350 and 500 K depending on the relative coverages of the reactants on the surface (5, 7). It has generally been concluded that this recombination step is fast as long as there are sufficient O and CO species on the surface; this is true for experiments with $CO + O_2$ (44) as well as with CO + NO (8, 10, 12–14, 16, 17, 27, 39). Fast decay and formation kinetics were observed here for CO_2 production from NO + CO under most steady-state conditions, as indicated by the almost immediate response of the CO_2 partial pressure to the blocking and unblocking of the beam.

4.2. *Rate-Limiting Step*

From the above discussions it appears that, except for atomic N recombination (step [8]), all other steps in the

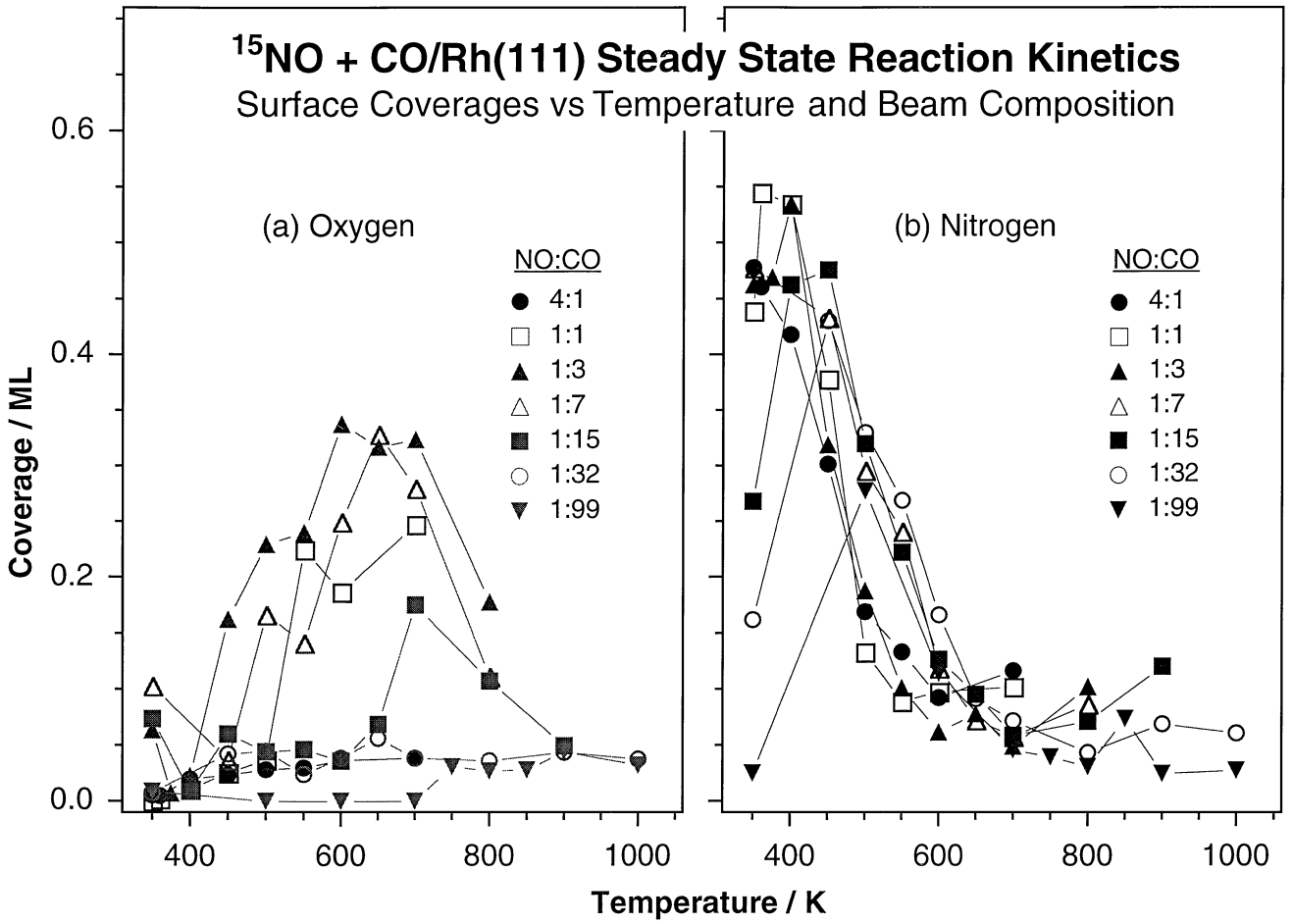

FIG. 11. Coverages of oxygen (a) and strongly adsorbed nitrogen (b) atoms under steady-state reaction conditions, as calculated from TPD data such as those in Figs. 8 and 9, as a function of reaction temperature for all the beam compositions employed in this report. Note that the nitrogen coverage decreases sharply with temperature, in approximately the same way for all $^{15}NO:CO$ ratios, while the oxygen coverage shows a more complex behavior, increasing with temperature (up to 700 K) and then decreasing again for intermediate beam compositions (for $^{15}NO:CO$ ratios between 1:1 and 1:7).

reaction mechanism are fast above 400 K. The almost immediate response of the CO_2 production trace to the blocking and unblocking of the molecular beam in particular attests to the fast nature of the NO dissociation reaction on the surface. This leaves nitrogen recombination as the most likely rate-limiting step for the overall NO + CO conversion under steady-state catalytic conditions, at least under vacuum (note that the total flux used in most of our experiments corresponds to pressures on the order of 1×10^{-6} Torr). Again, the slow response of the N_2 production trace to perturbations of the steady-state conditions provides direct evidence for such a conclusion. Unfortunately, the kinetics of the $N + N \rightarrow N_2$ step (and, therefore, of the overall NO conversion reaction) is complicated by the fact that there is a build-up of a critical N coverage on the surface before the beginning of any N_2 desorption. This was manifested here both by the delay in N_2 production in the transient state (Fig. 1) and by the large values of Θ_N^{strong} measured by TPD after reactions. The idea of a critical Θ_N^{strong} was already reported by us for the case of NO conversion by itself on Rh(111) (3), but the argument is better made in the NO + CO experiments because of the fast removal of the coadsorbed oxygen by CO there.

A discussion of the effect of nitrogen atoms on the reduction of NO over Rh(111) surfaces is the subject of a separate publication (34). Nevertheless, it is important to notice that there is no clear connection between the amount of the surface nitrogen detected by the TPD experiments and the rate of the NO + CO conversion. There is, if anything, an inverse correlation between Θ_N^{strong} and R for temperatures below about 600 K (Figs. 11 and 12), the opposite of what would be expected by using a simple rate law expression of the type $R = k_8 \cdot (\Theta_N^{strong})^{\alpha}$ for step [8]. Once again, we suggest that this is so because the majority of the adsorbed N atoms are not kinetically active, and are only needed to reach the starting point for the

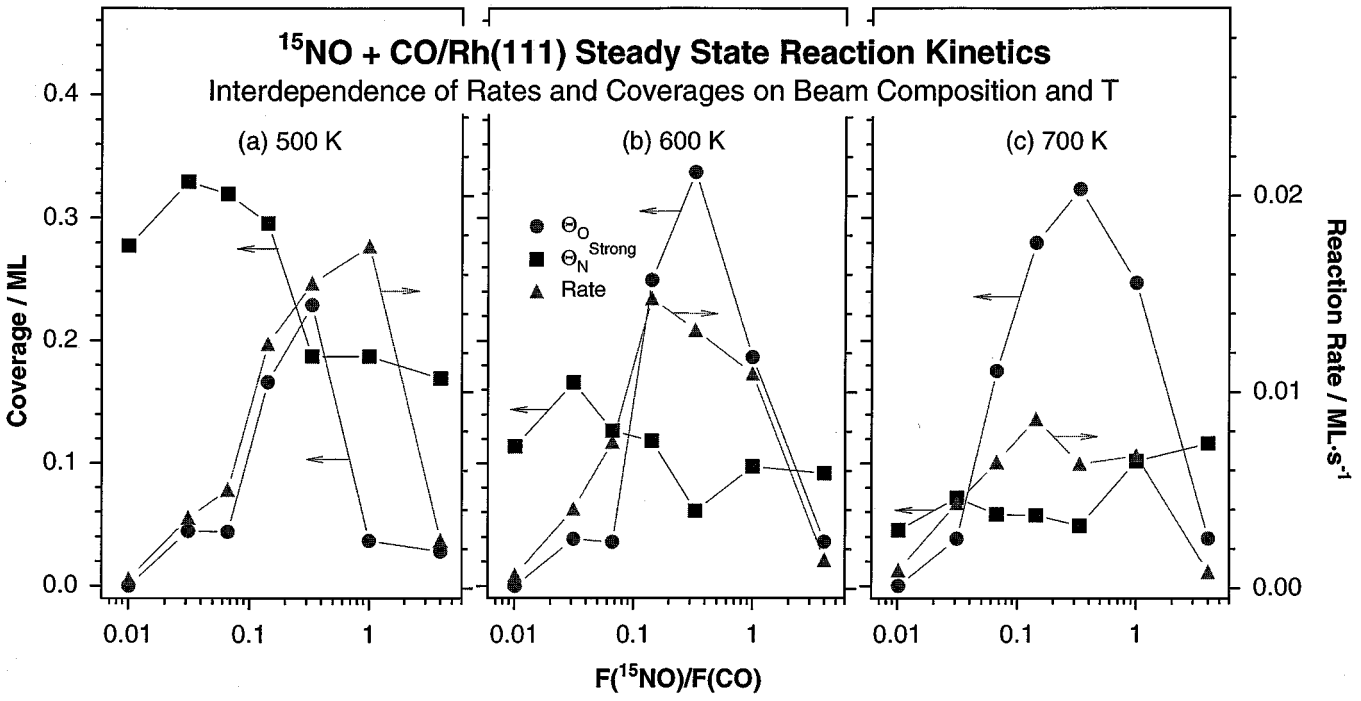

FIG. 12. Oxygen (circles) and nitrogen (squares) coverages and reaction rates (triangles) as a function of ^{15}NO : CO beam composition for 500 (a), 600 (b), and 700 K (c) reaction temperatures. A direct correlation is seen in most cases between oxygen coverages and reaction rates, while the presence of nitrogen atoms strongly held on the surface appears to poison the reaction instead.

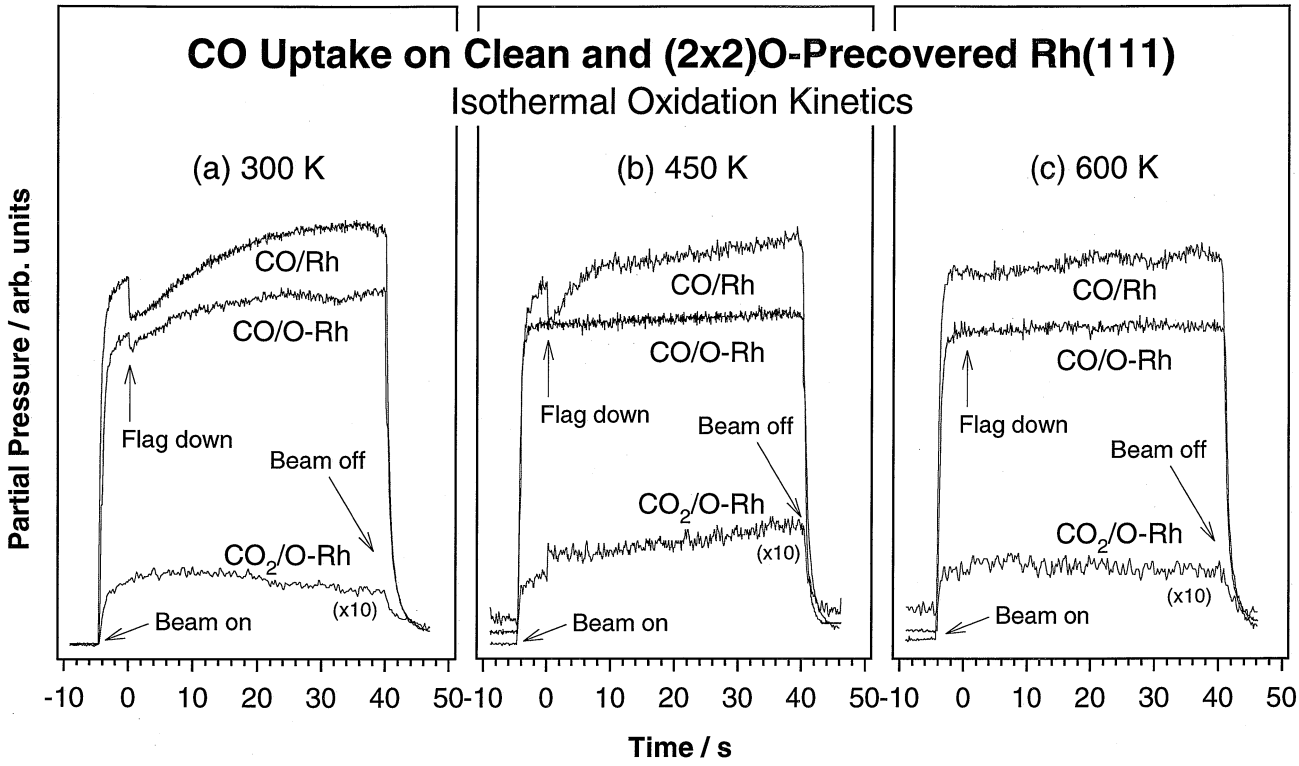

FIG. 13. Raw isothermal kinetic data for the uptake of CO on clean Rh(111) (top) and for both the uptake of CO (middle) and the evolution of CO_2 (bottom) on oxygen-covered Rh(111) surfaces at 300 (a), 450 (b), and 600 K (c). The rate of CO desorption is significantly higher than that of CO + O surface recombination at high temperatures.

desorption of N_2. This Θ_N^{strong} threshold is larger at lower temperatures regardless of beam composition, and also increases somewhat with increasing CO concentration in the beam (Fig. 12). We have previously explained these observations in terms of a strong repulsion among nitrogen (and/or oxygen) surface atoms (34), an effect that causes the activation energy for the nitrogen-recombination step to depend strongly on both Θ_N^{strong} and Θ_O (decreasing as the total surface coverage is increased) (3). Such a proposal is supported by the observation by Belton *et al.* of a shift in the atomic nitrogen recombination TPD peak from adsorbed NO toward high temperatures (by about 100 K) when in the presence of coadsorbed oxygen (26), and by a similar observation by Root *et al.* for the N_2 desorption from NO dissociation on clean versus CO-covered Rh(111) surfaces (5). It was also determined here that there is a small amount of additional nitrogen, Θ_N^{weak}, that adsorbs on the surface during the steady-state NO + CO reaction, and that $R \propto \Theta_N^{weak}$ (34).

4.3. Steady-State Kinetics

Additional analysis of our data provides further support for the mechanism presented at the beginning of this Discussion. The kinetic results refer to a steady-state regime for the NO + CO reaction, which means that the rates of steps [3] to [9] in that mechanism must reach equal values under a given set of conditions (temperature, beam flux, and beam composition). In that sense step [8], the recombination of atomic nitrogen, is considered rate limiting only because of the low value of its reaction rate constant; the rates of the other steps adjust under steady state via changes in the coverages of the different surface species. This implies that for steps with high reaction-rate constants, the coverages of their reactants display low steady-state values. We have already used this argument implicitly to conclude that the coverages of molecular CO and NO on the Rh(111) surface are low and in equilibrium with the gas phase because the rates of steps [3] to [6] are all high at the temperatures considered in this study.

The steady-state coverage of atomic oxygen during the NO + CO reaction, on the other hand, is detectable, and changes significantly with reaction conditions. The data that illustrate this fact are presented in Figs. 11 and 12. Figure 12 in particular shows that, for any given temperature, there is a good correspondence between Θ_O and R, at least in the case of NO-lean beams (NO : CO ≤ 1 : 3). This is consistent with a simple rate expression for step [9] of the form

$$R_{CO_2} = k_9 \cdot \Theta_{CO} \cdot \Theta_O, \qquad [10]$$

as long as Θ_{CO} remains approximately constant (because of the CO excess in the gas phase). There is also a direct correlation between the reaction rate and the NO beam flux (F_{NO}), presumably because under steady state Θ_O depends directly on the rate of step [7],

$$\Theta_O = \frac{k_7 \cdot \Theta_{NO}}{k_9 \cdot \Theta_{CO}} = \frac{k_7}{k_9} \cdot \frac{s_{NO}^0}{k_6 + k_7} \cdot \frac{\Theta_{vacant}}{\theta_{CO}} \cdot F_{NO}, \qquad [11]$$

so

$$R_{CO_2} = \frac{k_7 \cdot s_{NO}^0}{k_6 + k_7} \cdot \Theta_{vacant} \cdot F_{NO}. \qquad [12]$$

Notice that the proportionality between R_{CO_2} and F_{NO} is affected by changes in both the NO sticking coefficient and the concentration of vacant surface sites. In fact, blocking of empty sites by NO, N, and/or O is the reason for the poisoning of the reaction in the case of the NO-rich beams.

Figures 6 and 12 also illustrate how, in the 500 to 700 K range, the CO_2 and N_2 production rates decrease with temperature for a given beam composition. Given that the coverage of oxygen does not change significantly in that temperature range (Θ_O is about the same at 600 and 700 K, and, if anything, goes down at 500 K), this means that the steady-state coverage of CO on the surface must decrease with increasing temperature (see Eq. [10]). This is to be expected since, on the one hand, the sticking coefficient of CO on Rh(111) is high and almost temperature independent and, on the other, CO desorption is activated and therefore speeds up at higher temperatures. Notice also that, according to the data in Fig. 13, CO desorption is much faster than CO + O recombination, at least above 450 K, so the steady-state coverage of CO on the surface can be approximated to

$$\Theta_{CO} \cong \frac{s_{CO}^0 \cdot \Theta_{vacant} \cdot F_{CO}}{k_4} = \frac{s_{CO}^0}{k_4^0} \cdot \exp\left[\frac{E_{des,CO}}{RT}\right] \cdot \Theta_{vacant} \cdot F_{CO}, \qquad [13]$$

where $E_{des,CO}$, the activation energy for CO desorption, is on the order of 38 kcal/mol (32). Assuming a relatively insignificant change in Θ_{vacant} in the 500–700 K temperature range, Eq. [13] implies that Θ_{CO} should decrease exponentially with $1/T$.

4.4. Reaction Rate Maxima and Kinetics under Extreme Conditions

As mentioned in Results, a maximum in the rate of the reaction is generally observed at an optimum intermediate temperature for any given NO + CO beam composition, usually around 600 K (Fig. 6). This maximum is generally reached when the surface coverage of N atoms is low, $\Theta_N^{strong} \leq 0.1$ ML, and that of O is high, $\Theta_O \geq 0.2$ ML (Fig. 12). There is also a maximum rate at a fixed temperature for a given intermediate beam composition. This optimum beam is normally slightly rich in carbon monoxide. For instance, the maximum rate is obtained with a NO : CO ratio of 1 : 1 at 500 K, with a ratio of 1 : 3 at 550 K, and

with a ratio of 1 : 7 at 600 and 650 K. In connection with this, recall that at 350 K an equimolar surface mixture is obtained for an NO : CO ratio of about 1 : 7 in the gas phase (Fig. 10), and that NO adsorption competes even more favorably with that of CO at higher temperatures because of its higher adsorption energy. It is reasonable therefore to conclude that the NO + CO reaction proceeds faster when the coverages of NO and CO on the surface are near their 1 : 1 stoichiometric ratio, and that for a given beam composition the steady-state coverage of NO relative to that of CO increases with increasing surface temperature. This behavior explains the synergy between reaction temperature and beam composition mentioned in Results, Section 3.4.

Figure 6 also shows that the NO + CO conversion rate drops significantly when extreme conditions are used, namely, at low (below 450 K) or high (above 800 K) temperatures, and for CO-rich (NO : CO ratio below 1 : 30) and NO-rich (NO : CO ratios above 4 : 1) beams. Below 400 K the Rh(111) surface is in general saturated with reactant molecules, NO and CO (Figs. 10 and 11), and that poisons the NO + CO reaction (by blocking the decomposition of NO). Above 650 K, on the other hand, the nitrogen recombination step [8] is no longer rate limiting. Notice in particular the fast response of the N_2 trace after blocking of the beam during the steady-state experiments (Fig. 3). The onset temperature where the response of the N_2 production trace to changes in the beam is as fast as that for CO_2 increases with decreasing NO concentration in the beam (Fig. 5). Moreover, both Θ_N^{strong} and Θ_O are quite low at high temperatures, something not expected from the high sticking coefficients for NO seen on clean Rh(111) up to 800 K (3). Three points are to be considered here: (1) Some CO and O_2 desorbs above 1100 K during the TPD experiments following high-temperature reactions, and the remaining oxygen appears to diffuse into the Rh bulk. In fact, XPS and SSIMS studies of the thermal chemistry of NO on Rh(111) suggest that a small amount of O atoms diffuse slowly into the subsurface above 600 K (45–47). (2) Figures 9 and 11 indicate that Θ_O drops rapidly between 700 and 800 K even in experiments with NO-rich beams, hinting that the NO adsorption–desorption equilibrium (steps [5] and [6] shifts towards the gas phase at these temperatures. (3) The CO-titration TPD data (Fig. 9) show the development of a new CO_2 desorption state about 360 K not seen for reaction temperatures below 600 K, indicating the presence of O atoms adsorbed in a different arrangement (most likely forming oxygen islands (36, 37)). Finally, the experiments with NO-rich (4 : 1 ratio of NO : CO) and CO-rich (1 : 99 ratio of NO : CO) beams show low rates at all temperatures (Fig. 5). We attribute this mainly to the high coverage of the excess reactant, at least up to 600 K. The large Θ_N^{strong} threshold required to initiate the N recombination step [8] below 600 K provides an additional explanation for the low rate seen at low temperatures.

4.5. Comparison with Previous Results

This report adds a few new and perhaps controversial ideas to the discussion of the NO + CO/Rh(111) system. As mentioned in the Introduction, the extensive work by the group at General Motors has already provided much knowledge on this subject. In their earlier studies of this process under high pressures, Fisher *et al.* suggested a very high coverage of N atoms ($\Theta_N = 0.96$ and 0.99 ML at 500 and 675 K, respectively), which led them to the conclusion that N_2 desorption must be the rate-limiting step of the whole process (18). Later on, however, the same group assumed nitrogen desorption to be fast, and the N coverage on the surface to always remain below 0.35 ML (8). Their new model predicted that at low P_{NO}/P_{CO} ratios the overall NO reduction rate may be limited by the CO + O oxidation step, at least at lower temperatures. Last, the idea was put forward that at least one channel for N_2 formation was via the reaction of N with NO adsorbed species (4, 5, 7–9, 24).

Belton and co-workers (10, 11, 17, 26, 27) revised those ideas in several ways. First, they measured the rate for N recombination independently, and concluded that such a step may not be rate limiting, at least when Θ_N is large. Second, they proved that no disproportionation between NO(ads) and N(ads) to produce N_2 ever takes place; instead the two reactants may only recombine to produce gaseous N_2O. Third, they indicated that at high NO pressures (>2 Torr) N_2 formation is always accompanied by the production of an equal or larger amount of N_2O below 700 K: higher selectivity towards N_2 was observed above 600 K at low P_{NO} ($\leq$0.8 Torr), but the yield for the NO to N_2 conversion was always below 15% in their studies. Fourth, they reported that with equimolar reactants of NO and CO the Rh(111) surface is mainly covered by NO species between 500 and 700 K (21), but that under an excess of gas-phase CO its coverage on the surface increases with increasing temperature. Based on all this the authors proposed that NO dissociation is the rate-limiting step for the overall NO + CO reaction under atmospheric pressures.

A comparison of our results with those of Belton *et al.* suggests that somewhat different mechanisms may be operative at UHV and under high pressures, or at least that the relative contribution of the different elementary steps to the kinetics of the overall reaction changes between the two regimes. For one, no N_2O is produced under UHV, as is the case at atmospheric pressures. We interpret this in terms of a change in NO coverage on the surface as a function of gas pressure: under vacuum the steady-state population of NO is so low that atomic nitrogen recombination to N_2 dominates any possible N + NO reaction, but this may no longer be true in the atmospheric pressure range. Molecular beam work using high fluxes is planned in our laboratory to address this point. Also, it was shown here that the

preferential adsorption of NO over CO on the rhodium surface is favored by higher, not lower, temperatures.

A new and important observation from the results presented in this paper is that there is a build-up of a critical coverage of nitrogen atoms on the Rh surface before N_2 production starts. As already explained above, our evidence points to N_2 desorption as the rate-limiting step of the overall NO reduction process. The fast initial formation of CO_2 at the beginning of our kinetic runs and the fast response of the CO_2 rate to changes in the beam flux under steady-state conditions unequivocally tells us that NO dissociation and CO_2 formation are faster than N_2 production under most reaction conditions. On the other hand, because of the complex kinetic behavior of the N_2 production step seen here, the high Θ_N values reported by Belton *et al*. do not necessarily translate into fast N recombination rates. These points had not been brought out by any previous studies, partly because little direct evidence has been available on the kinetics of the individual reaction steps prior to this molecular beam work. Our experiments were performed under vacuum, but are likely to reproduce many of the features of the processes that occur under the more realistic catalytic converter conditions.

5. CONCLUSIONS

This paper reports the results from a kinetic study on the NO + CO reaction over Rh(111) single-crystal surfaces for a wide range of F_{NO}, F_{CO}, and temperatures. The experiments were carried out isothermally and under ultra-high vacuum by using collimated effusive collimated beams, but were performed under conditions where the NO reduction reaction could be sustained in a catalytic regime similar to that encountered in realistic catalytic converters. Analysis of the kinetic data led to the conclusion that under most conditions the rate of the overall process is limited by the diffusion-controlled surface recombination of nitrogen atoms on the surface. Two types of kinetically different adsorbed nitrogen atoms were detected on the surface, as apparent by the build-up of a critical coverage of nitrogen atoms before N_2 production begins. This critical Θ_N^{strong} coverage decreases with increasing temperatures and decreasing oxygen coverages, and does not correlate directly with the reaction rates. An additional small coverage of more reactive nitrogen atoms is responsible for the N_2 formation on the surface.

It was also found that there is an optimum reaction temperature for a given NO + CO beam composition which maximizes the steady-state rate of the NO reduction. That maximum in reaction rate shifts to higher temperature with increasing CO concentration in the reaction mixture. Conversely, there is an optimum NO : CO ratio that maximizes the overall rate at a given temperature. This optimum ratio changes with reaction temperature but is always centered around the stoichiometric mixture. The synergy between temperature and beam composition was explained here in terms of the effect of those parameters on the relative steady-state concentrations of the NO and CO adsorbed on the surface. Finally, significant deviations from the optimum rates were observed when the reactions were carried out under extreme conditions. At low temperatures, below 400 K, the surface becomes saturated with a mixture of species, molecular NO and CO in particular, and the reaction is poisoned because of the inhibition of the NO dissociation step. On the high-temperature side, above 800 K, the rate appears to be limited by the short residence time of CO on the surface and also by oxygen diffusion into the bulk. Finally, deviations from the stoichiometric reaction mixture result in poisoning by the excess reactant.

ACKNOWLEDGMENTS

Funding for this research was provided by a grant from the National Science Foundation (CTS-9812760). We thank Dr. David N. Belton for the donation of the Rh(111) single crystal as well as for his helpful discussions.

REFERENCES

1. Taylor, K. C., *Catal. Rev. Sci. Eng.* **35**, 457 (1993).
2. Shelef, M., and Graham, G. W., *Catal. Rev. Sci. Eng.* **36**, 433 (1994).
3. Aryafar, M., and Zaera, F., *J. Catal.* **175**, 316 (1998).
4. Root, T. W., Schmidt, L. D., and Fisher, G. B., *Surf. Sci.* **134**, 30 (1983).
5. Root, T. W., Schmidt, L. D., and Fisher, G. B., *Surf. Sci.* **150**, 173 (1985).
6. Zhdanov, V. P., and Kasemo, B., *Surf. Sci. Rep.* **29**, 31 (1997).
7. Root, T. W., Fisher, G. B., and Schmidt, L. D., *J. Chem. Phys.* **85**, 4687 (1986).
8. Schwartz, S. B., Fisher, G. B., and Schmidt, L. D., *J. Phys. Chem.* **92**, 389 (1988).
9. Peden, C. H. F., Goodman, D. W., Blair, D. S., Berlowitz, P. J., Fisher, G. B., and Oh, S. H., *J. Phys. Chem.* **92**, 1563 (1988).
10. Peden, C. H. F., Belton, D. N., and Schmieg, S. J., *J. Catal.* **155**, 204 (1995).
11. Belton, D. N., and Schmieg, S. J., *J. Catal.* **144**, 9 (1993).
12. Dubois, L. H., Hansma, P. K., and Somorjai, G. A., *J. Catal.* **65**, 318 (1980).
13. Becker, W. C., and Bell, A. T., *J. Catal.* **84**, 200 (1983).
14. Hendershot, R. E., and Hansen, R. S., *J. Catal.* **98**, 150 (1986).
15. Cho, B. K., Shanks, B. H., and Bailey, J. E., *J. Catal.* **115**, 486 (1989).
16. Cho, B. K., *J. Catal.* **148**, 697 (1994).
17. Ng, K. Y. S., Belton, D. N., Schmieg, S. J., and Fisher, G. B., *J. Catal.* **146**, 394 (1994).
18. Oh, S. H., Fisher, G. B., Carpenter, J. E., and Goodman, D. W., *J. Catal.* **100**, 360 (1986).
19. Oh, S. H., and Carpenter, J. E., *J. Catal.* **101**, 114 (1986).
20. Oh, S. H., *J. Catal.* **124**, 477 (1990).
21. Permana, H., Ng, K. Y. S., Peden, C. H. F., Schmieg, S. J., Lambert, D. K., and Belton, D. N., *J. Catal.* **164**, 194 (1996).
22. DeLouise, L. A., and Winograd, N., *Surf. Sci.* **159**, 199 (1985).
23. Borg, H. J., Reijerse, J. F. C.-J. M., van Santen, R. A., and Niemantsverdriet, J. W., *J. Chem. Phys.* **101**, 10052 (1994).
24. Root, T. W., Fisher, G. B., and Schmidt, L. D., *J. Chem. Phys.* **85**, 4679 (1986).
25. Kao, C.-T., Blackman, G. S., Van Hove, M. A., Somorjai, G. A., and Chan, C.-M., *Surf. Sci.* **224**, 77 (1989).

26. Belton, D. N., DiMaggio, C. L., and Ng, K. Y. S., *J. Catal.* **144**, 273 (1993).
27. Belton, D. N., DiMaggio, C. L., Schmieg, S. J., and Ng, K. Y. S., *J. Catal.* **157**, 559 (1995).
28. Gopinath, C. S., and Zaera, F., *J. Phys. Chem.*, submitted for publication.
29. Liu, J., Xu, M., Nordmeyer, T., and Zaera, F., *J. Phys. Chem.* **99**, 6167 (1995).
30. Öfner, H., and Zaera, F., *J. Phys. Chem.* **101**, 396 (1997).
31. Weissler, G. L., and Carlson, R. W., Eds., "Vacuum Physics and Technology." Academic Press, New York, 1979.
32. Thiel, P. A., Williams, E. D., Yates, J. T., Jr., and Weinberg, W. H., *Surf. Sci.* **84**, 54 (1979).
33. Zaera, F., Liu, J., and Xu, M., *J. Chem. Phys.* **106**, 4204 (1997).
34. Zaera, F., and Gopinath, C. S., *J. Chem. Phys.*, submitted for publication.
35. Bugyi, L., and Solymosi, F., *Surf. Sci.* **258**, 55 (1991).
36. Matsushima, T., Matsui, T., and Hashimoto, M., *J. Chem. Phys.* **81**, 5151 (1984).
37. Thiel, P. A., Yates, J. T., Jr., and Weinberg, W. H., *Surf. Sci.* **82**, 22 (1979).
38. Liu, J., Xu, M., and Zaera, F., *Catal. Lett.* **37**, 9 (1996).
39. Campbell, C. T., and White, J. M., *Appl. Surf. Sci.* **1**, 347 (1978).
40. Biberian, J. P., and Van Hove, M. A., *Surf. Sci.* **138**, 361 (1984).
41. Dubois, L. H., and Somorjai, G. A., *Surf. Sci.* **91**, 514 (1980).
42. Crowell, J. E., and Somorjai, G. A., *Appl. Surf. Sci.* **19**, 73 (1984).
43. Peterlinz, K. A., Curtiss, T. J., and Sibener, S. J., *J. Chem. Phys.* **95**, 6972 (1991).
44. Schwartz, S. B., Schmidt, L. D., and Fisher, G. B., *J. Phys. Chem.* **90**, 6194 (1986).
45. van Hardeveld, M., Ph.D. thesis, Technische Universiteit Eindhoven, 1997.
46. Wider, J., Greber, T., Wetli, E., Kreutz, T. J., Schwaller, P., and Osterwalder, J., *Surf. Sci.* **417**, 301 (1998).
47. Peterlinz, K. A., and Sibener, S. J., *J. Phys. Chem.* **99**, 2817 (1995).